

Complexation in a 5-acylpyrimidine-4-thione—aliphatic diamine—metal(II) chloride system (M = Ni or Co). The molecular structure of *fac*-tris(5-acetyl-2,4-dimethylpyrimidine-6-thiolato)cobalt(III)

E. K. Beloglazkina,* A. A. Chizhevskii, V. N. Nuriev, R. L. Antipin, N. V. Zyk, I. V. Chernyshev, A. A. Moiseeva, and K. P. Butin†

Department of Chemistry, M. V. Lomonosov Moscow State University,
1 Leninskie Gory, 119992 Moscow, Russian Federation.
E-mail: bel@org.chem.msu.su

The reactions of 5-acylpyrimidine-4-thiones with aliphatic diamines in the presence of Ni^{II} and Co^{II} salts were studied. New Ni^{II} and Co^{III} complexes with ligands of the pyrimidinethione series were synthesized. The results of the reactions of 5-acetyl-6-methyl-2-phenylpyrimidine-4-thione and 5-acetyl-2,6-dimethylpyrimidine-4-thione with ethylenediamine or 1,3-diaminopropane in the presence of NiCl₂·6H₂O or CoCl₂·6H₂O depend on (1) the nature of the substituent at position 2 of the pyrimidine ring, (2) the length of the polymethylene bridge between the nitrogen atoms in the diamine molecule, (3) the nature of complex-forming metal, and (4) the pyrimidinethione : diamine ratio. The resulting complexes were studied by electrochemical methods. The mechanism of electrooxidation and electroreduction of 5-acylpyrimidine-2-thiones and related nickel and cobalt complexes was proposed. The structures of the complexes were investigated by NMR, UV-Vis spectroscopy, and IR spectroscopy and mass spectrometry. The molecular structure of *fac*-tris(5-acetyl-2,4-dimethylpyrimidine-6-thiolato)cobalt(III) was established by X-ray diffraction. According to semiempirical quantum-chemical calculations by the PM3(tm) method, both the highest occupied and lowest unoccupied molecular orbitals in the molecules of the compounds under study have a π symmetry and are localized predominantly on the ligand fragments.

Key words: 5-acylpyrimidine-4-thiones, nickel(II), cobalt(II), cobalt(III), transition metal complexes, electrochemistry, molecular structure.

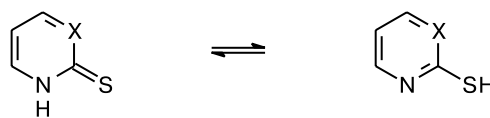
Recently,¹ we have reported the synthesis and the results of physicochemical study of nickel complexes with N₂S₂-type imine-containing ligands, which are thiosalen analogs. The aim of the present study was to synthesize complexes of heterocyclic analogs of thiosalen containing the thio-substituted pyrimidine fragment. Thiopyrimidines possess a broad spectrum of physiological and biological activities. Some modern drugs contain metal ions coordinated by pyridine-2-thiones (see Ref. 2 and references therein). Complexes of pyrimidine- and pyridine-2-thiones can also be considered as model compounds in studies of the chemical properties of 6-thioguanosine (2-amino-1,2-dihydro-3β-D-ribofuranosyl-6H-purine-6-thione).³ The behavior of nickel complexes can simulate the mechanisms of action of the active sites of particular hydrogenases (in which the Ni ion is in a distorted octahedral or square-planar coordination environment formed by N,S-containing ligands^{4–7}).

2-Thio-substituted pyridines and 2- or 4-thio-substituted pyrimidines exist in two tautomeric forms, *viz.*,

† Deceased.

thione and thiol (see, for example, Scheme 1 for 2-substituted derivatives).

Scheme 1



X = CH, N

In the crystalline state, all known monothio-substituted derivatives of pyridines and pyrimidines exist in the thione form.⁸ There are data⁹ that the thiol form prevails in nonpolar solvents and the gas phase. However, according to other data,¹⁰ monomeric thiones rather than thiols are present even in dilute nonpolar solvents.

Complexation with metals is generally accompanied by deprotonation of pyridine- and pyrimidinethiones.⁸ However, complexes with neutral ligands were also documented.¹¹ Numerous of pyridine- and pyrimidinethiolate

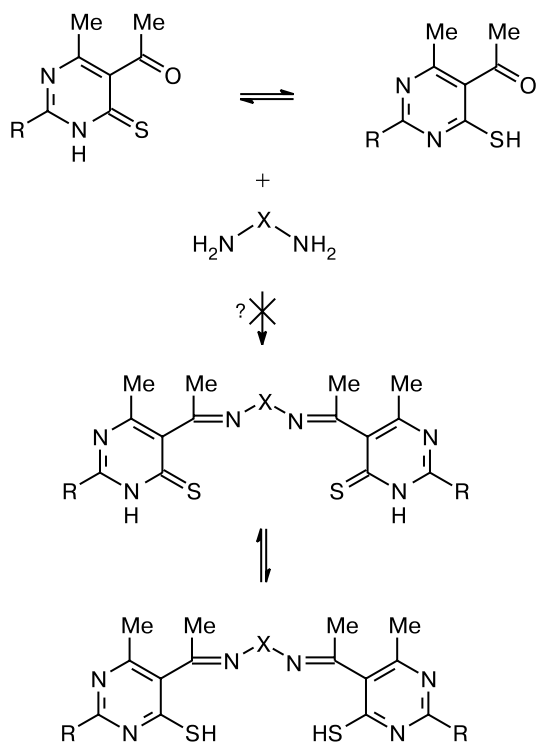
complexes with both transition and main-group metals were described in the literature (see, for example, the reviews^{8,12}).

Heterocyclic thiolates (thionates) exhibit ambident properties (serve as N- or S-monodentate ligands in complexes with Hg^{II},¹³ Au^I (see Ref. 14) and Fe^{II}, Co^{II}, and Ni^{II} (see Reg. 15)). However, in most complexes, these compounds serve as bidentate ligands. In S,N-chelated complexes, the metal ion is coordinated by heterocyclic thionate to form a four-membered metallacycle.⁸

Results and Discussion

Although complexation of 2-pyridine- and 2-pyrimidinethiones has been studied in detail, complexation of their derivatives containing additional coordinating atoms remained unknown. In the present study, we examined the possibility of preparing tetradentate ligands containing two 2-pyrimidinethione fragments and two imine groups, which can coordinate the transition metal ion through the nitrogen atom. We expected that the reaction of 5-acylpyrimidine-4-thione with aliphatic diamines would afford the bis(iminothione) ligands (Scheme 2).

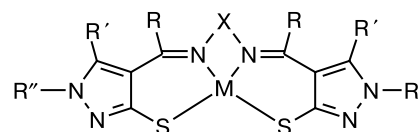
Scheme 2



R = Ph (**1**), Me (**2**); X = (CH₂)₂, (CH₂)₃

Both the starting thione and this ligand can exist as thiol-thione tautomers and can be involved in complexes

in either the neutral or deprotonated form. Data on complexes of imino-substituted pyridine- or pyrimidinethiones are lacking. Cobalt¹⁶ and copper^{17–21} complexes based on imino-substituted imidazolylthiolates are the most structurally similar compounds. All complexes of this type synthesized so far contain the ligand in the deprotonated thiol form.



M = Co, Cu

Our attempts to synthesize free ligands by the reaction shown in Scheme 2 with the use of different conditions (by refluxing reagents in ethanol, with the use of benzene–water azeotropic distillation, or in DMF; in the presence of catalytic amounts of acids (acetic, hydrochloric, or *p*-toluenesulfonic) or bases (triethylamine or piperidine); or by varying the acylpyrimidinethione : diamine ratio (2 : 1 or 1 : 1)) failed.

However, the addition of nickel or cobalt chloride hexahydrate to the reaction mixture and refluxing for 10–30 min led to the formation of complexes as colored powdered precipitates.

We studied the reactions of 6-methyl-2-phenyl- (**1**) and 5-acetyl-2,6-dimethylpyrimidine-4-thione (**2**) with ethylenediamine and 1,3-diaminopropane in the presence of Ni^{II} and Co^{II} salts using various combinations of three starting reagents. It appeared that the structures of the complexes formed in the three-component reactions depend on the following factors: (1) the nature of the substituent at position 2 of the pyrimidine ring, (2) the length of the polymethylene bridge between the nitrogen atoms in the diamine molecule, (3) the type of complex-forming metal, and (4) the pyrimidinethione : diamine ratio. The colors, the melting points, and elemental analysis data for the complexes are given in Table 1. Depending on the conditions used, the reactions afforded complexes, which can be assigned to four structural types: iminothiolate complexes **3** and **4** containing the ligand in the deprotonated form, iminothione complexes **5** and **6** containing the neutral organic ligand, keto thiolate complex **7**, and complexes **8** and **9** containing deprotonated ligand **1**, chloride anions, and diamine.

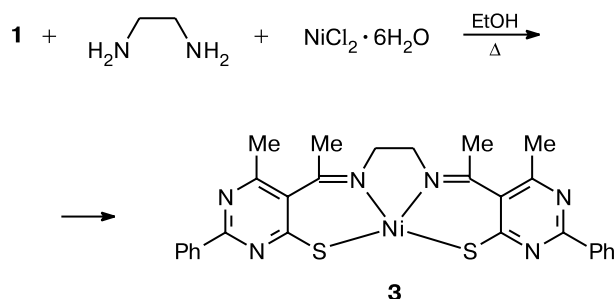
If the starting compound contains the phenyl substituent at position 2 of the pyrimidine ring, ethylenediamine (eda) is used as the amine component of condensation, and compound **1** and eda are taken in a ratio of 2 : 1, the reaction affords gold-beige diimino dithiolate complex **3** in ~40% yield (Scheme 3). An increase in the reaction time (to 12 h) has no substantial effect on the yield of compound **3**.

Table 1. Physicochemical characteristics and elemental analysis data for complexes 3–9

Com-plex	Method of preparation	Color	M.p. /°C	Found / Calculated (%)			Molecular formula
				C	H	N	
3	A	Gold-beige	285–290 (decomp.)	58.50 59.04	5.15 4.60	14.89 14.76	C ₂₈ H ₂₆ N ₆ NiS ₂
4	A	Gold-beige	160–162	58.40 57.43	4.30 4.48	13.59 14.36	C ₂₈ H ₂₆ CoN ₆ OS ₂
5	A	Brown-red	284–285 (decomp.)	52.73 52.36	4.57 4.39	12.80 13.08	C ₂₈ H ₂₈ Cl ₂ N ₆ NiS ₂
6	A	Light-green	290 (decomp.)	37.99 37.78	6.12 5.26	14.00 14.69	C ₂₉ H ₃₆ Cl ₂ N ₆ NiO ₃ S ₂
7	A	Dark-green	218	44.65 47.83	4.29 4.52	12.76 13.95	C ₂₄ H ₂₇ CoN ₆ O ₃
8*	B	Pale-green	>350	47.84 45.32	5.52 4.82	15.57 14.09	C ₁₅ H ₁₉ ClN ₄ NiOS
9**	B	Brown-green	>300	47.98 47.16	4.52 4.20	13.75 13.75	C ₁₆ H ₁₇ ClN ₄ NiOS

* Found (%): Ni, 16.09. Calculated (%): Ni, 16.05.

** Found (%): Cl, 8.54. Calculated (%): Cl, 8.70.

Scheme 3

The results of studies of the complexes with pyrimidine-containing ligands by electronic and IR spectroscopy are summarized in Table 2. The results of mass spectrometry are given in Table 3.

The ¹H NMR spectrum of complex 3 shows signals for the aromatic protons at δ 8.40–7.45, singlets for the protons of the methyl groups at δ 2.30 and 2.45, and a broadened singlet for the protons of the CH₂N groups at δ ~1.5. The absence of signals for the thioamide proton in the ¹H NMR spectrum of complex 3 indicates that ligand 1 in this complex is deprotonated. The fact that it is possible to record the NMR spectrum is evidence that the resulting compound is diamagnetic, *i.e.*, the Ni^{II} ion (d⁸) in complex 3 is in the low-spin state, which can occur only in a square-planar coordination environment. This is also confirmed by the presence of a low-intensity absorption band in the electronic spectrum of 3 at λ = 400 nm. The IR spectrum of complex 3 shows an absorption band of the imino group at 1680 cm⁻¹ (for comparison, the carbonyl group of the starting pyrimidinethione 1 is observed in

Table 2. UV–Vis and IR spectroscopic data for ligands 1 and 2 and complexes 3–9

Com- pound	IR, ^a ν/cm ⁻¹	UV–Vis, ^b λ/nm (ε/L mol ⁻¹ cm ⁻¹)
1	1700, 2900 (br), 3170	—
2	1700, 2900 (br), 3175	—
3	1470, 1500, 1530, 1680	278 (38400), 400 (3600)
4	1470, 1510, 1540, 1680	— ^c
5	1410, 1680, 3170, 3230	— ^d
6	1460, 1520, 1550, 1680, 3050 (br), 3480	304 (13980)
7	1515, 1550, 1685, 1700	304 (18820)
8	1520, 1705, ~3200 (br), 3305, 3380	—
9	1525, 1550, 1700, ~3200 (br), 3305, 3380	—

^a In Nujol mulls.

^b In DMF, 10⁻³ mol L⁻¹.

^c No absorption bands are observed at λ ≥ 270 nm.

^d The complex is poorly soluble in DMF.

the IR spectrum at 1700 cm⁻¹). This is indicative of the absence of conjugation between the carbonyl group and the pyrimidine ring in the starting compound and the presence of conjugation, *i.e.*, flattening of the system, in the case of formation of the imine bond and complexation with metal. The IR spectrum shows no bands at 2800–3500 cm⁻¹ (except for C–H stretching bands), which additionally confirms the deprotonated state of the pyrimidine fragment in complex 3.

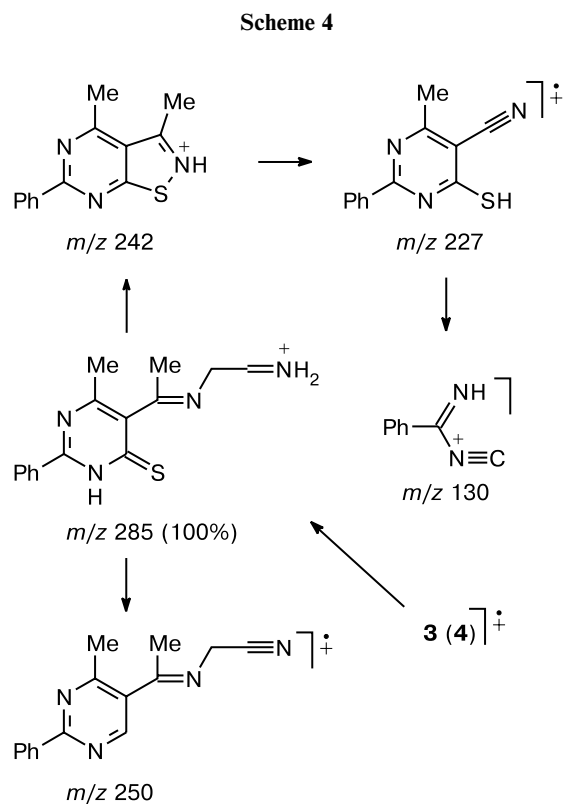
The molecular ion peak is absent in the mass spectrum of compound 3 (direct inlet, electron impact). How-

Table 3. Results of MALDI-TOF mass-spectrometric analysis

Compound	m/z (I (%))	
	Main peaks ($I > 15\%$)	Selected low-intensity peaks ($I = 3-10\%$)
3*	130 (17), 250 (32), 285 (100), 509 (15)	227 (10), 242 (10)
4	130 (17), 227 (15), 285 (100), 509 (15)	242 (10), 250 (10), 487 (3), 584 [$1/2 M^+ - H$] (3), 729 (3), 730 (3), 753 (3)
6	130 (45), 136 (30), 285 (100), 316 (17)	227 (7), 242 (10), 250 (9), 617 [$M^+ - Cl$] (3), 652 [M^+] (4)
8	130 (100), 243 (70), 361 [$M^+ - Cl$] (30)	620, 644, 768
9	243 (100)	461, 474, 487

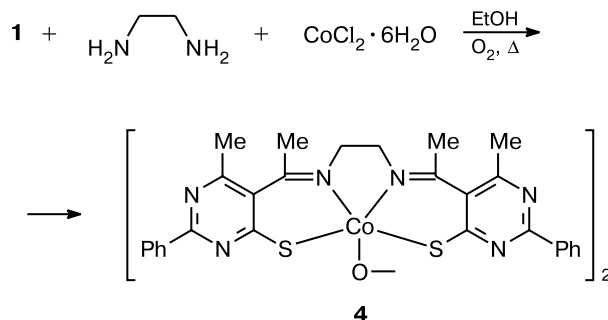
* Electron-impact ionization.

ever, the presence of fragment ion peaks at m/z 285 ($C_{15}H_{17}N_4S$), 250 ($C_{15}H_{14}N_4$), 242 ($C_{13}H_{12}N_3S$), and 227 ($C_{12}H_9N_3S$) corresponding to the structure presented in Scheme 4 confirms the presence of the imine bond in the ligand. The possible fragmentation pathways are shown in Scheme 4.



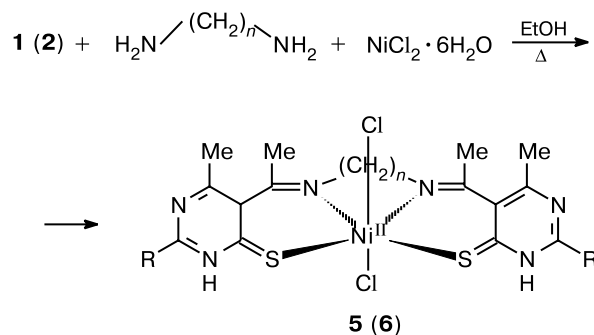
An analogous reaction with cobalt chloride produces gold-beige compound **4**, to which the structure of the Co^{III} imino thiolate complex was assigned (Scheme 5).

Apparently, atmospheric oxygen serves here as an oxidizer because the reaction performed in a nitrogen atmosphere does not give complex **4**.

Scheme 5

The 1H NMR and IR spectra of compound **4** are very similar to the corresponding spectra of complex **3**. This is evidence that these compounds are structurally similar. At the same time, diamagnetism of complex **4** (the possibility of recording the NMR spectrum) indicates that this complex contains Co^{III} . According to the elemental analysis data and the Beilstein test, chlorine atoms are absent in compound **4**. The main fragmentation pathway in the MALDI-TOF mass spectrum of complex **4** is analogous to that of complex **3** (see Scheme 4). The mass spectrum shows also low-intensity signals at m/z 584 [$1/2 M^+ - H$] and at m/z 729, 730, and 753, i.e., peaks of ions whose masses are larger than those of the possible mononuclear cobalt complexes. Based on these data, we assigned an oxygen-bridged dimeric structure to complex **4** (see Scheme 5).

The reaction of pyrimidinethione **1** with 1,3-diaminopropane and the reaction of pyrimidinethione **2** with eda in the presence of nickel chloride (the pyrimidinethione : diamine ratio was 2 : 1) afforded (Scheme 6) complexes **5** and **6**, respectively, which are, apparently, derivatives of diimines of the pyrimidinethione series.

Scheme 6

5: R = Ph, $n = 3$; **6:** R = Me, $n = 2$

The NMR spectra are uninformative for the determination of the structures of complexes **5** and **6**. The lines in the spectra are strongly broadened, which indicates that the nickel atom is paramagnetic. Apparently, compounds **5** and **6** belong to octahedral high-spin Ni^{II} complexes (see Scheme 6). This is consistent with the results of electronic spectroscopy. No intense absorption bands are in the visible region of the spectrum at the maximum achievable concentration of 10⁻³ mol L⁻¹ for a solution of compound **5**, whereas ϵ for octahedral Ni^{II} complexes are usually close to the possible lower limit (0–10). The IR spectra of complexes **5** and **6**, like the spectra of complexes **3** and **4**, show bands at ~1680 cm⁻¹ belonging to vibrations of the imino group. In addition, the spectrum of complex **5** shows medium-intensity bands at 3170 and 3230 cm⁻¹, which can be assigned to N–H stretching vibrations of the thioamide fragment.

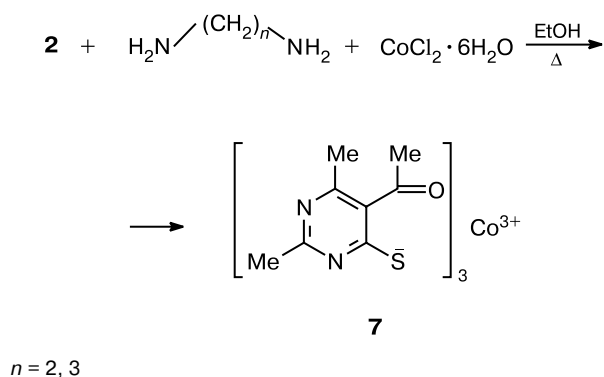
The fragmentation in the mass spectrum (MALDI) of complex **6** is similar to that observed for imine-containing complexes **3** and **4**. The main peaks in the spectrum of **6** belong to the ions formed upon bond cleavage in the γ position with respect to the imino group (m/z 285 (C₁₆H₁₉N₃S) and 250 (C₁₆H₁₆N₃)) and signals at m/z 242, 227, and 130.

A positive Beilstein test confirms the presence of chloride anions in complexes **5** and **6**.

It should be noted that polymeric bridged structures of complexes **5** and **6** are also cannot be ruled out, as evidenced by low solubility of these compounds in organic solvents being studied.

Under the same conditions, the reaction of dimethyl-substituted pyrimidinethione **2**, NiCl₂·6H₂O, and 1,3-diaminopropane does not afford a complex. An analogous reaction of compound **2** with a Co^{II} salt produces cobalt(III) tris-keto thiolate **7** regardless of the nature of diamine (Scheme 7).

Scheme 7



Evidently, atmospheric oxygen serves as an oxidizer. The reaction in pre-deoxygenated ethanol under an argon

Table 4. Principal crystallographic characteristics of compound **7**

Parameter	Characteristic
Molecular formula	Co(C ₈ H ₉ N ₂ OS) ₃
Molecular weight	602.63
Crystal system	Orthorhombic
Space group	<i>Pna</i> 2 ₁
<i>a</i> /Å	21.168(2)
<i>b</i> /Å	17.509(2)
<i>c</i> /Å	7.4140(7)
<i>V</i> /Å ³	2747.8(5)
<i>Z</i>	4
ρ_{calc} /g cm ⁻³	1.457
$\mu(\text{Cu-K}\alpha)$ /cm ⁻¹	7.342
Angle range/deg	3.28–65
Crystal dimensions/mm	0.10×0.05×0.03
Number of reflections in least-squares	4625
Number of parameters in refinement	344
<i>R</i> ₁ [<i>I</i> > 2 σ (<i>I</i>)]	0.0456
<i>wR</i> ₂	0.1328

atmosphere did not afford complex **7**; instead, the brown-beige Co(eda)₂Cl₂ complex was obtained.

The structure of complex **7** was established by X-ray diffraction. The crystallographic characteristics and details of X-ray diffraction study are given in Table 4. Selected interatomic distances and bond angles are listed in Table 5. The molecular structure of compound **7** is shown in Fig. 1. The cobalt atom in complex **7** is in a distorted *fac*-octahedral coordination environment formed by the S and N(1) atoms of three pyrimidine ligands giving rise to three strained four-membered rings. Molecule **7** can be described as a three-blade propeller consisting of three ligand fragments. The acetyl substituent at position 5 of the pyrimidine rings is not conjugated with the π -system of the six-membered ring (the angle between the plane of the pyrimidine ring and the C=O group averaged over three ligands is 29(2)°). A similar *fac* structure has been

Table 5. Selected interatomic distances (*d*) and bond angles (ω) for compound **7** (the atomic numbering scheme is given in Fig. 1)

Bond	<i>d</i> /Å	Angle	ω /deg
Co–N(1A)	1.975(5)	N(1A)–Co–S(1A)	72.05(16)
Co–N(1B)	1.984(5)	N(1B)–Co–S(1B)	72.13(16)
Co–N(1C)	1.979(5)	N(1C)–Co–S(1C)	72.45(16)
Co–S(1A)	2.255(2)	N(1A)–Co–N(1B)	102.3(2)
Co–S(1B)	2.247(2)	N(1A)–Co–N(1C)	100.4(2)
Co–S(1C)	2.2529(19)	N(1A)–Co–S(1B)	91.92(17)
S(1A)–C(2A)	1.725(6)	N(1A)–Co–S(1C)	164.38(17)
S(1B)–C(2B)	1.738(7)	N(1C)–Co–S(1B)	167.34(15)
S(1C)–C(2C)	1.736(7)	N(1B)–Co–S(1A)	167.03(16)
N(1A)–C(2A)	1.353(8)	C(2A)–S(1A)–Co	79.7(2)
N(1B)–C(2B)	1.357(8)	C(2A)–N(1A)–Co	100.2(4)
N(1C)–C(2C)	1.362(8)	N(1A)–C(2A)–S(1A)	107.9(4)

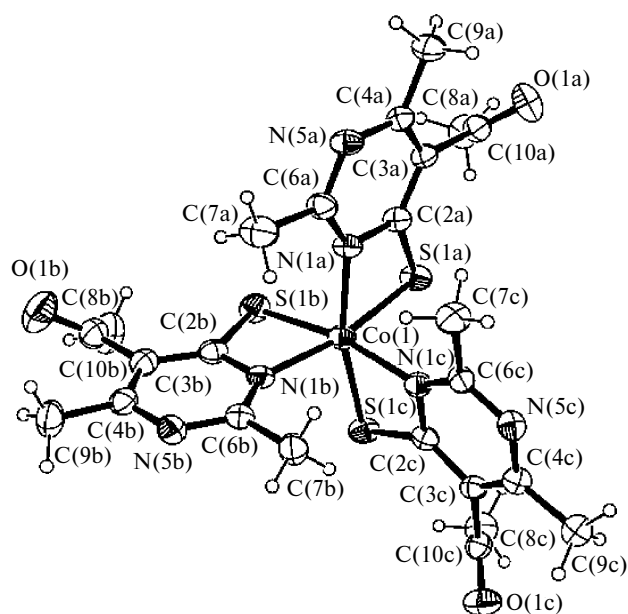


Fig. 1. Molecular structure of complex **7**. The atoms are represented by anisotropic displacement ellipsoids drawn at the 30% probability level.

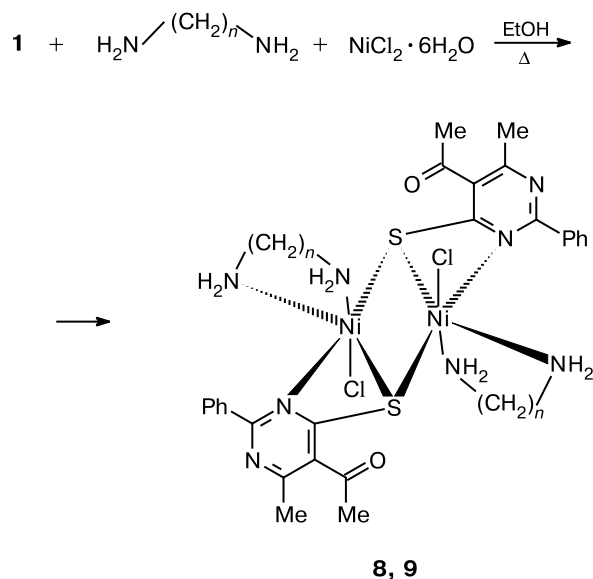
established earlier^{22,23} in the X-ray diffraction study of cobalt(III) tris(4,6-dimethylpyrimidin-2-thionate). By contrast, the analogous Co^{III} 2-pyridinethionate complex has a meridional structure.^{24,25} It was hypothesized²⁶ that the complex adopts either a facial or meridional configuration depending on the steric and electronic factors, the *fac* isomer being more stable among low-spin d⁶-tris-chelates. In the case of tris-chelates of heterocyclic thionates, the S...S interactions are the strongest, whereas the interligand interactions are the weakest in the *fac* isomer. The opposite is true for the meridional isomer. Apparently, the *fac* isomer is favorable for substituted pyrimidinethionate ligands in spite of the presence of the S...S nonbonded interaction (the distances between the S atoms in complex **7** are 3.29–3.35 Å).

The C–N and C–S bond lengths in the ligand are similar to the corresponding single bond lengths, which is typical of complexes of this type.⁸ In all ligands, the pyrimidine and chelate rings are almost coplanar (the average dihedral angle between these fragments is 4(1)°). The virtually planar structures of the four-membered chelate rings show that this system is moderately strained.

The reaction with the use of a different ratio of the starting reagents (pyrimidinethione **1**, diamine, and the nickel salt) were taken in a ratio of 1 : 1 : 1 afforded complexes **8** and **9** (Scheme 8) with the molecular formula $\{(LH)NiCl[H_2N(CH_2)_mNH_2]\}_n$ ($L = \mathbf{1}$, $m = 2$ or 3). Complexes **8** and **9** are paramagnetic (it was impossible to record the NMR spectra of these complexes). Hence, the square-planar configuration can be rejected. The presence of the amine and carbonyl groups in both complexes

is proved by the fact that their IR spectra show bands at 3200–3380 and 1700 cm⁻¹, the latter being analogous to the absorption band of the starting pyrimidinethione **1**. Compounds **8** and **9** contain chloride anions, which is confirmed by a positive Beilstein test (for complex **9**, the presence of chloride anions was confirmed also by elemental analysis data). The main peak in the MALDI-TOF mass spectra of complexes **8** and **9**, unlike that in the spectra of imine complexes **3**, **4**, and **6**, is observed at m/z 243 and corresponds to the ion $[\mathbf{1} - H]^+$ (see Table 3). In addition, the spectrum has low-intensity peaks corresponding to ions whose masses are larger than those of mononuclear nickel complexes. Taking into account these data, bridged dimeric structures (see Scheme 8) analogous to those described earlier¹² seem to be the most probable structures. The possibility of the existence of such structures containing bridging sulfur atoms and metal ions in a nearly octahedral coordination environment was confirmed by quantum-chemical calculations of the geometric parameters of complex **8** (see below). However, polymer structures of complexes **8** and **9** cannot be ruled out.

Scheme 8



$n = 2$ (**8**), 3 (**9**)

Electrochemical study. Complexes **3–9** and 5-acylpyrimidinethione **2** were studied by cyclic voltammetry (CV) and rotating disk electrode (RDE) voltammetry on glassy-carbon (GC), Pt, and, in some cases, Au electrodes in DMF solutions in the presence of 0.05 M Bu₄NClO₄ as the supporting electrolyte. The electrochemical oxidation and reduction potentials are given in Table 6.

Table 6. Electrochemical reduction potentials (E^{Red}) and oxidation potentials (E^{Ox}) of the complexes with pyrimidine-containing ligands measured relative to Ag|AgCl|KCl(sat.) by the CV (E_p is the peak potential) and RDE ($E_{1/2}$ is the half-wave potential) methods at a glassy-carbon electrode^a

Compound	E_p^{Red}	$E_{1/2}^{\text{Red}}$	E_p^{Ox}	
			$E_{1/2}^{\text{Ox}}$	
V				
2	-1.73	-1.71 (1)	1.53	1.52 (2)
	-2.27	-2.21 (1)		
3	-1.36 ^b	-1.32 (2)	1.46	1.39 (2)
	-2.28			
4	-1.18	-1.18 (~3)	—	—
	-2.31	-2.28 (2)		
5	-1.37	-1.24 (2)	1.17	1.24 (2)
	-0.06 ^{c,d}			
6	-2.28			
	-1.52	-1.34 (2)	1.26	1.16 (2)
7	-0.05 ^{c,d}			
	-1.90			
8	-1.80	-0.46 ^e	1.61	1.58 (2)
	-1.55	-1.23 (2)	1.26	1.30 (2)
9	-0.0 ^{c,d,f}	-1.80 (2) ^g		
	-2.16			
NiCl ₂ ·6H ₂ O	-1.52	-1.25 (2)	1.24	1.34 (2)
	-0.06 ^{c,d,f}			
NiCl ₂ ·6H ₂ O	-2.30			
	-1.32	-1.30 (2)	1.20	1.00 (2)
	+0.16 ^c			

^a Experimental conditions: DMF, 0.05 M Bu₄NClO₄; CV, 200 mV s⁻¹; RDE, 20 mV s⁻¹; 2800 min⁻¹. The numbers of electrons transferred in the step, which were determined on a rotating disk electrode by comparing with the one-electron oxidation wave of ferrocene, are given in parentheses. For comparison, the table also gives the oxidation and reduction potentials of NiCl₂·6H₂O.

^b On a GC electrode, the peak was split into two components; no splitting of the peak is observed on a Pt electrode.

^c The peak potential in the reverse scan of the CV curve.

^d The reverse peak corresponding to desorption of Ni⁰ increases with accumulation at the potential of the first reduction wave.

^e The number of electrons transferred during reduction of **7** cannot be determined because of broadening of the peaks in the RDE curve followed by a decrease in the current.

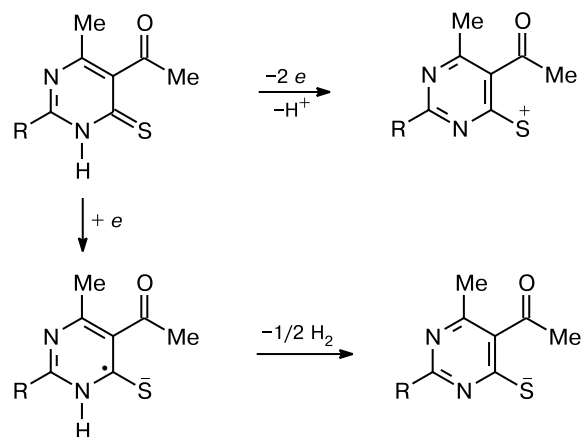
^f Both peaks are shifted with time to lower cathodic potentials.

^g On a Pt electrode.

5-Acylpyrimidinethione **2** is reduced successively in two one-electron steps, whereas its oxidation occurs in one two-electron step (see Table 6). We performed semiempirical quantum-chemical calculations by the PM3 method.²⁷ These calculations demonstrated that both the highest occupied and lowest unoccupied molecular orbitals (HOMO and LUMO, respectively) in molecules **1** and **2** have a π symmetry, the orbital patterns being virtually independent of whether the calculations are carried out for the thiol or thione form. The orbitals of the sulfur

lone pair make the major contribution to HOMO, whereas the conjugated π -system of the pyrimidine ring makes the major contribution to LUMO (Fig. 2). These results suggest that oxidation of the ligands occurs primarily at the sulfur-containing fragment, whereas the pyrimidine fragment is predominantly subjected to reduction. The resulting radical cation or radical anion contains a hydrogen atom, which can be abstracted. Hence, oxidation presumably generates the corresponding pyrimidine-containing cation, whereas reduction produces the thiolate ion (Scheme 9).

Scheme 9



Quantum-chemical calculations by the PM3(tm) method for complexes **3**–**8** demonstrated that the symmetry of the frontier orbitals in these complexes is analogous to that of the corresponding orbitals of pyrimidinethiones **1** and **2**. Thus, HOMO are localized on the sulfur atoms (thiolate or thione), whereas LUMO are localized on the pyrimidineimine fragment (see Fig. 1). In none of the cases, was a significant contribution of the orbitals of the metal atom to the frontier orbitals observed. This suggests that the initial electronic changes in all the complexes synthesized should occur at the ligand fragments. It should be noted that the calculated geometric parameters of complex **7** agree well with those determined by X-ray diffraction. Calculations with geometry optimization also gave the *fac* isomer. The calculated bond lengths are similar to those determined experimentally. According to calculations, the carbonyl group is not conjugated with the π system of the pyrimidine fragment. For complex **3**, the calculated geometry of the coordination environment of the metal atom is almost square-planar, which is consistent with the results of electronic spectroscopy (see above). Therefore, quantum-chemical calculations by the PM3(tm) method, on the whole, adequately predict both the geometry and electron distribution for complexes of the pyrimidinethione series.

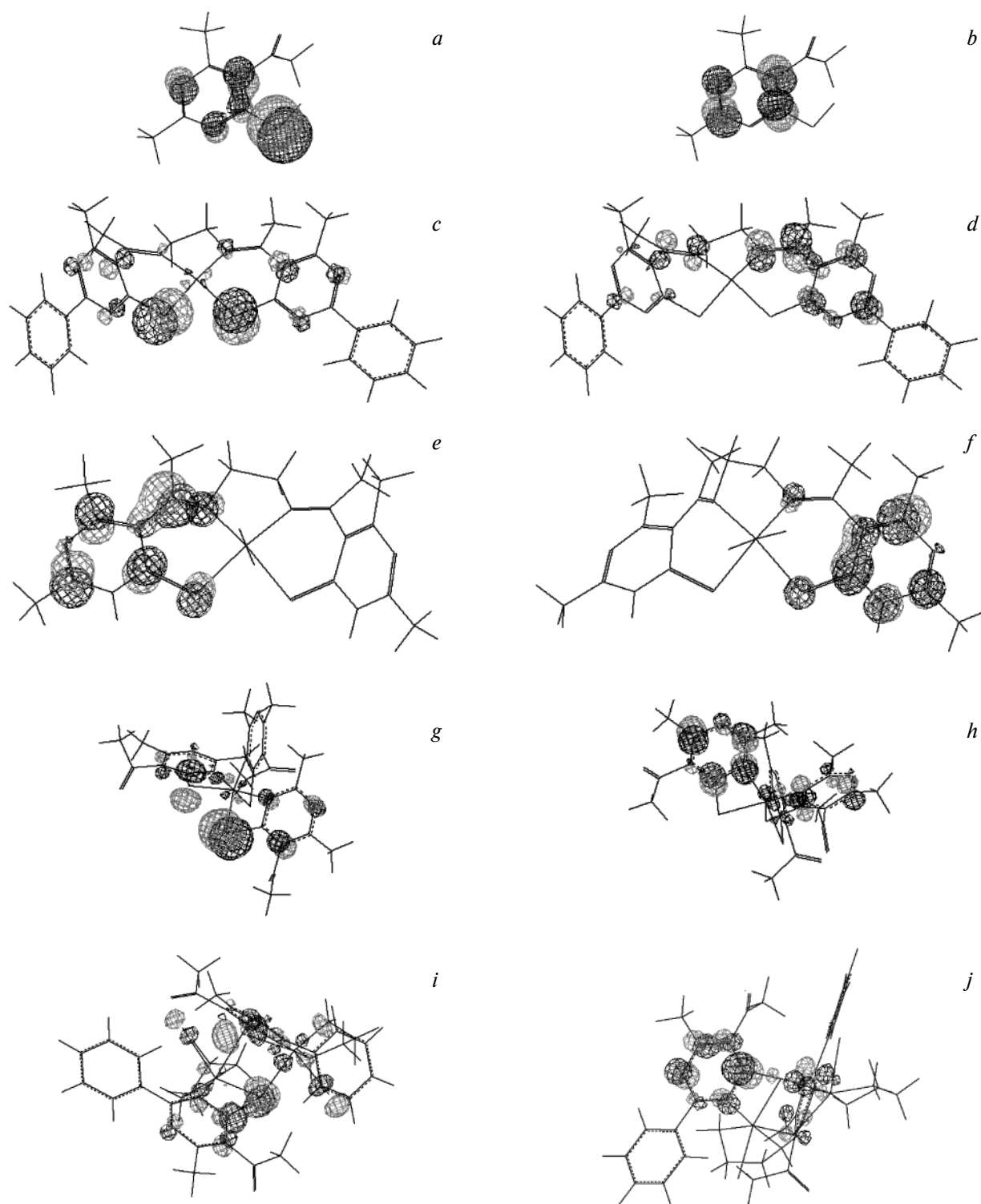


Fig. 2. Frontier orbitals of the thiol form of pyrimidinethione **2** (*a, b*) and complexes **3** (*c, d*), **6** (*e, f*), **7** (*g, h*), and **8** (*i, j*) calculated by the PM3(tm) method: HOMO (*a, c, e, g, i*) and LUMO (*b, d, f, h, j*).

The complexes under consideration can be divided into two types according to their electrochemical behavior in the cathodic region in DMF solutions. In the first step of reduction of complexes belonging to the

first type (compounds **3**, **4**, and **7**), decomposition of the complexes with elimination of zerovalent metal does not occur. Complexes with ligands in the deprotonated thiolate form and containing no chlorine atoms

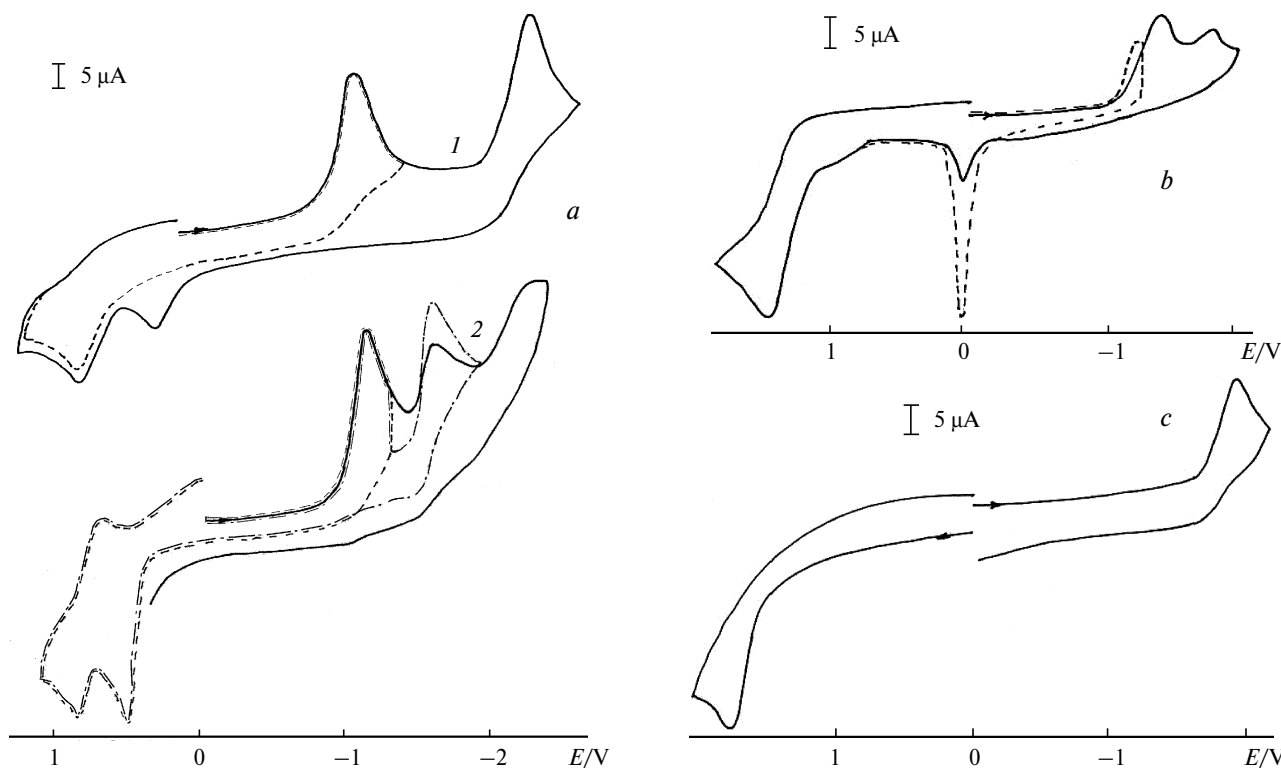


Fig. 3. Cyclic voltammograms (DMF, 0.05 M Bu₄NClO₄) of *a*, complex **4** ($5 \cdot 10^{-4}$ mol L⁻¹) in the absence of BuⁱI (*1*) and in the presence of an excess ($5 \cdot 10^{-2}$ mol L⁻¹) of BuⁱI (*2*), *b*, complex **6** ($3 \cdot 10^{-4}$ mol L⁻¹), *c*, complex **7** ($3 \cdot 10^{-4}$ mol L⁻¹).

(Fig. 3, *a*, *c*) belong to this type. Complexes of the second type (**5**, **6**, **8**, and **9**) containing chloride anions are characterized by the irreversible two-electron first reduction step accompanied by deposition of metallic Ni on the electrode surface. This is evidenced by the appearance of a characteristic peak of oxidative desorption of Ni⁰ at $E \sim 0$ V in the reverse potential scan (see Fig. 3, *b*). The intensity of this peak increases with increasing electrolysis time at the potential of the first reduction wave.

The identification of oxidation and reduction products of the complexes was beyond the scope of the present study. Nevertheless, taking into account the orbital patterns (see Fig. 2) and the above-described experimental data, the electrooxidation and electroreduction mechanisms can be proposed (Schemes 10–14).

Reduction of iminothiolate complex **3** occurs in two one-electron irreversible steps (see Fig. 3, *a*). Once the potential of the first wave in the CV curve is achieved, the desorption peak of Ni⁰ is not detected in the reverse potential scan. However, a low-intensity peak ($E = +0.5$ V) appears after the achievement of the potential of the second wave. The calculated bond orders in dianion **3** correspond to the structure **B** (see Scheme 10).

Two-electron oxidation of complex **3** should occur at the sulfur atoms giving rise, apparently, to a disulfide bond between two closely-spaced sulfur atoms. This is

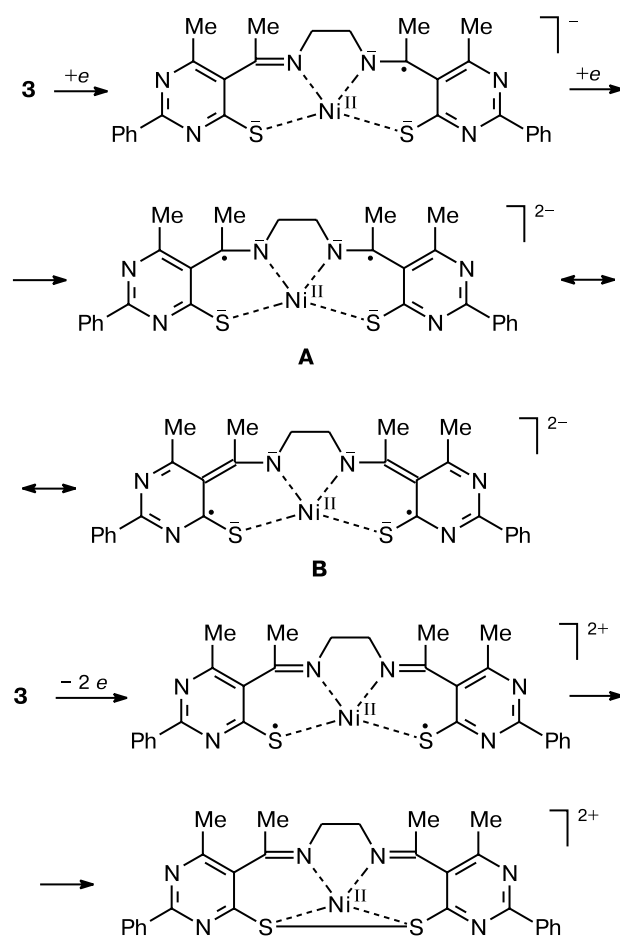
confirmed by calculations. In neutral complex **3**, the S–S distance is 2.84 Å, whereas this distance in dication **3**²⁺ is 2.38 Å, which is smaller than twice the van der Waals radius of the sulfur atom.

Oxidation of complex **4** is not accompanied by the appearance of peaks in the anodic region of the CV curve up to the potential $E_p = 1.7$ V. Apparently, the complex is oxidized at higher anodic potentials.

Reduction of complex **4** occurs in two irreversible steps at $E_p = -1.18$ and -2.31 V. The height of the first peak is higher than the level corresponding to the two-electron transfer, whereas the second peak corresponds to a two-electron process. During the reverse anodic scan after the achievement of the potential of the first wave, a peak at $E_p = 0.72$ V appears. After the achievement of the potential of the second reduction step, a reoxidation peak of Co⁰ appears at $E_p = 0.19$ V. The intensity of the latter peak slightly increases with increasing electrolysis time at a potential of -2.31 V.

Upon the addition of an excess of BuⁱI to a solution of **4** (see Fig. 3, *a*, curve 2), a new peak ($E_p = -1.64$ V) appears already during the first cathodic potential scan, and the intensity of the peak increases with increasing electrolysis time at the potential of the first reduction peak of compound **4**. During the reverse potential scan, an oxidation peak of the iodide anion²⁸ ($E_p = +0.48$ V) appears in the anodic region.

Scheme 10



The proposed mechanism of the processes occurring during reduction of complex **4** is shown in Scheme 11. The initial two-electron reduction of **4**, like that of complex **3**, occurs at the pyrimidineimine fragment. However, complex **4**, unlike **3**, can then decompose (by analogy with that described in the studies^{29,30}) to form the neutral LCo^{II} complex (see Scheme 7) and the peroxide dianion characterized by a reoxidation peak in the anodic region at +0.72 V.^{29,30} The resulting divalent cobalt complex undergoes disproportionation to give Co^{I} and Co^{III} complexes ($[\text{LCo}^{\text{I}}]^-$ and $[\text{LCo}^{\text{III}}]^+$, respectively).

Instability of Co^{II} complexes with some nitrogen-containing ligands and their disproportionation have been discussed, for example, in the publications.^{31,32} The $[\text{LCo}^{\text{III}}]^+$ complex should be reduced in the same potential region, where the starting complex **4** is reduced, which is responsible for the observed increase in the cathodic current of the first reduction peak. The pathways of transformations of $[\text{LCo}^{\text{I}}]^-$ depend on the presence or absence of an alkylating agent in the solution. In the absence of $\text{Bu}^{\text{n}}\text{I}$ (pathway *b*), this complex undergoes further reduction to form the dianion, which can be described either as

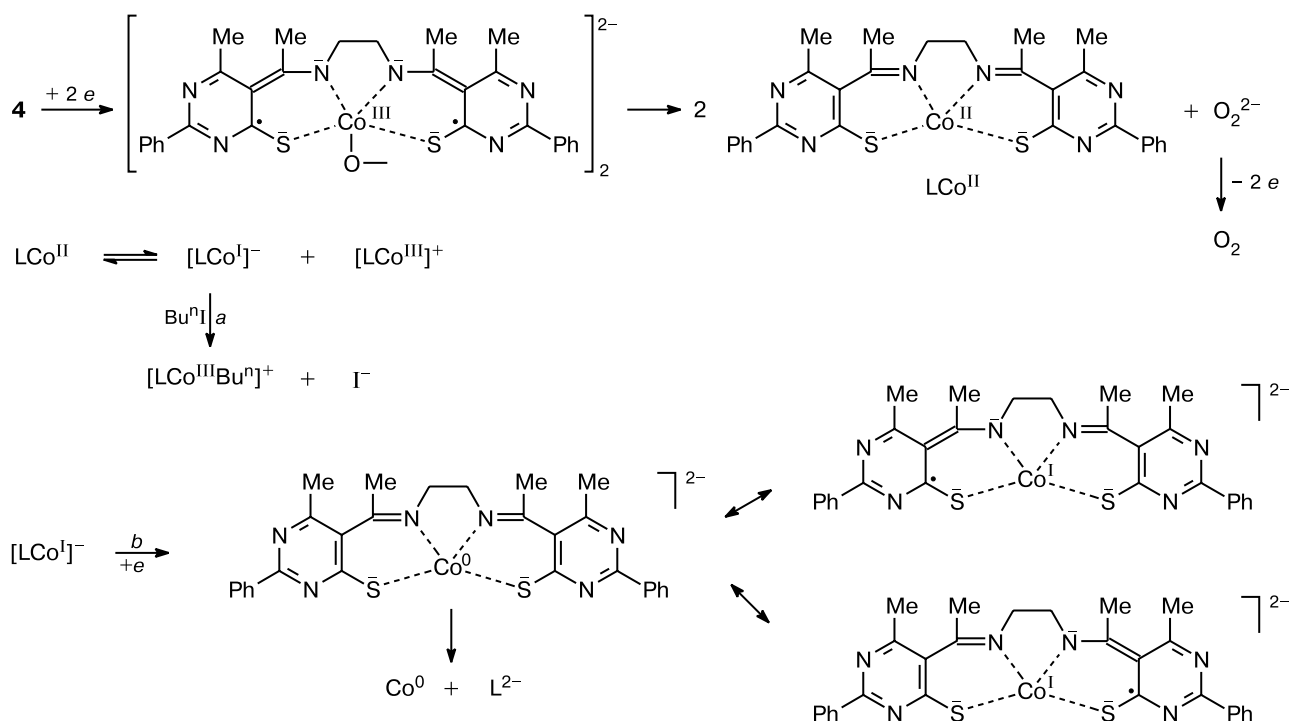
a Co^0 complex with the dianionic ligand or as a Co^{I} complex with the trianionic ligand. Scheme 11 shows three possible resonance structures of this dianion.

In the presence of $\text{Bu}^{\text{n}}\text{I}$ (pathway *a*), the $[\text{LCo}^{\text{I}}]^-$ anion can undergo alkylation to give the $[\text{Co}^{\text{III}}\text{Bu}^{\text{n}}]^+$ compound.

The reduction peak at $E_p = -1.85$ V and the oxidation peak at $E_p = 1.61$ V with an intensity ratio of 1 : 2 are observed in the CV curves of complex **7**. According to quantum-chemical calculations, the electron transfer processes occur here predominantly at the ligand fragment. However, unlike other complexes, compound **7** is, apparently, strongly adsorbed on the electrode surface. This is evidenced by the following data. A potential scan from 0 V to the oxidation region gives rise to an additional peak in the CV curves prior to the main anodic peak. This is an adsorption peak because its intensity (i_p) linearly depends on the scan rate (v) in the range of 20–1000 mV s^{-1} . The formation of an adsorption peak before the normal peak characterizes strong adsorption of the starting compound.³³ This is confirmed by the presence of a hysteresis in the CV curve (an Au electrode) during the reverse potential scan after the peak at $E_p = -1.85$ V. At a low potential scan rate (20 mV s^{-1}), a broad low-intensity peak was observed by rotating disk electrode voltammetry in the cathodic region at potentials of -0.45 – 1.35 V with the use of all the electrodes under study (GC, Pt, or Au). In the anodic region, the oxidation curve was observed only on a glassy-carbon rotating disk electrode, $2e$. On Pt and Au electrodes, a peak is observed instead of the "normal" two-electron wave. Since the voltammograms measured on rotating disk electrodes are anomalous both for oxidation and reduction (the anomaly increases on an Au electrode, where sulfur-containing complexes are involved in adsorption processes), the neutral starting complex is, presumably, adsorbed. Apparently, this is attributed to the fact that molecule **7** contains three closely-spaced thiolate fragments, which are attached to the electrode surface to form an Au–S or Pt–S bond (see, for example, Ref. 34).

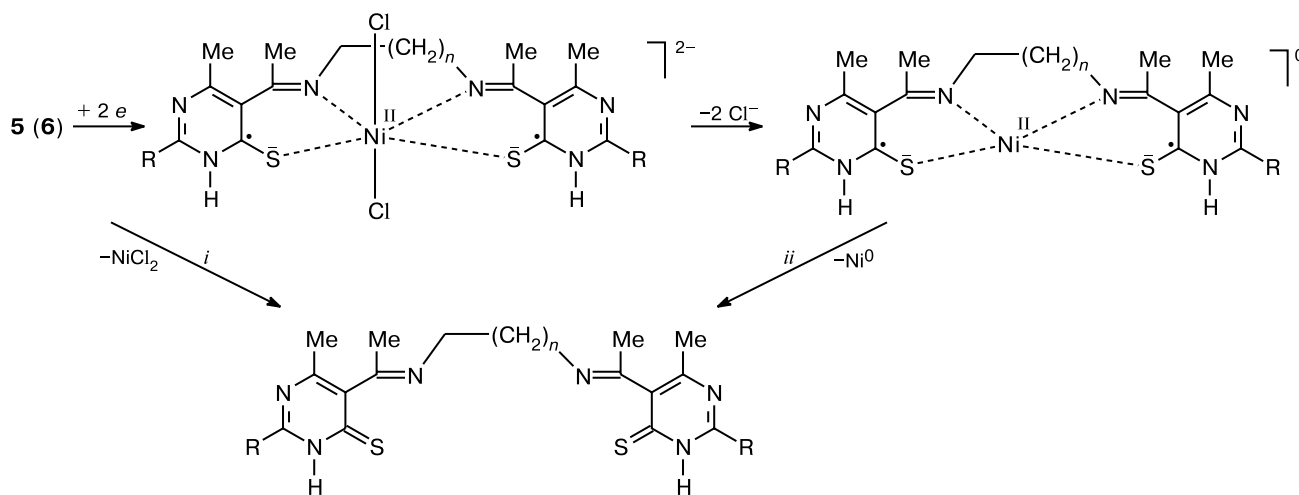
Complexes of the second type containing chloride anions undergo two-electron reduction in the first step with deposition of metallic nickel on the electrode surface. For compounds **5** and **6**, a reoxidation peak of Ni^0 , which appears after the first cathodic potential scan, is small. However, the intensity of this peak sharply increases with increasing electrolysis time at the potential of the first step. It should be noted that the color of the solution of complex **5** in DMF changes with time from orange to yellow-green. Within 10–15 min after dissolution of compounds **5** and **6**, an additional peak appears at -1.30 V, which is characteristic of reduction of NiCl_2 (see Table 6). The mechanism of oxidation and reduction of compounds **5** and **6**, which was proposed taking into account the results of quantum-chemical calculations, is shown in

Scheme 11



Conditions: *a*. In the presence of Bu^nI ; *b*. In the absence of Bu^nI .

Scheme 12

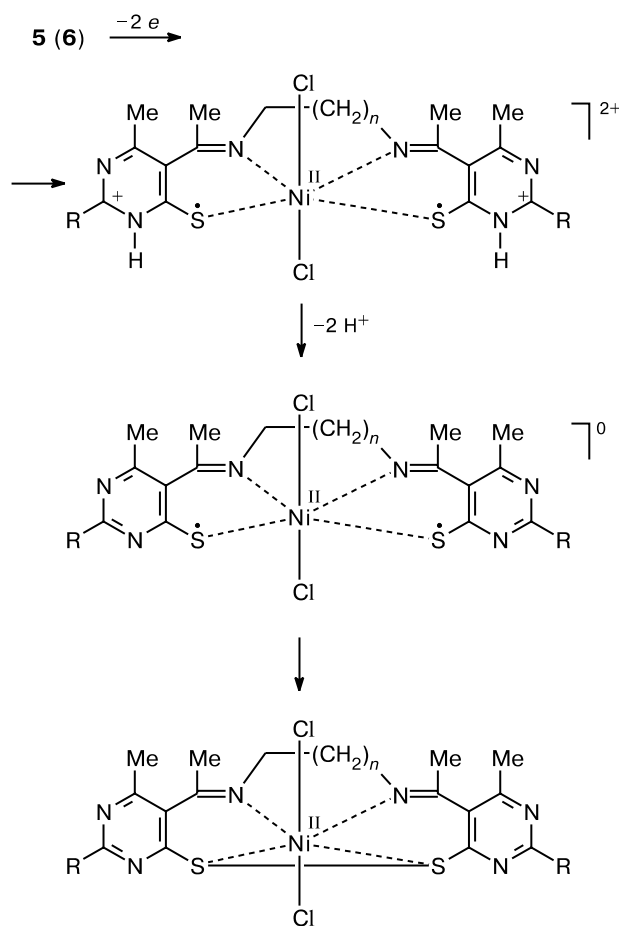


i. Slowly; *ii*. Rapidly.

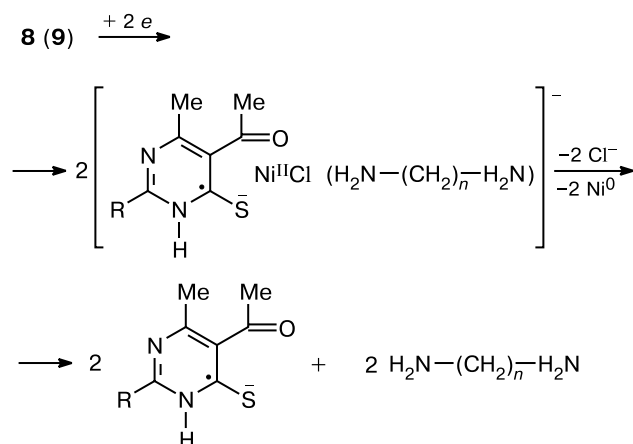
Scheme 12. Presumably, the dianion formed upon two-electron reduction eliminates two chloride anions (in the anodic region, an oxidation peak of Cl^- appears at 1.2 V, and the intensity of this peak increases with increasing electrolysis time), and the resulting neutral complex decomposes to form metallic nickel and bis(imino-

pyrimidinethione). At the same time, the appearance of the reduction peak of NiCl_2 upon storage of solutions of the complexes without electrolysis and the observed change in the color in the case of compound 5 indicate that the complexes with ligands of this type slowly dissociate in DMF to give nickel chloride and the free ligand

Scheme 13



Scheme 14



in the absence of the electric current as well. Therefore, the changes in the CV curves observed in solutions of the iminothione-type complexes can be explained taking into account that the following two processes occur: fast elimination under the action of NiCl_2 complexes upon reduc-

tion and slow elimination upon storage of the solution. Apparently, the second peak observed at cathodic potentials corresponds to reduction of bis(iminopyrimidinethione) that is generated taking into account that its potential is similar to the reduction potential of pyrimidinethione **2** (see Table 6).

Presumably, two-electron oxidation (see Scheme 13) affords a complex with the disulfide ligand (the calculated S—S distance in the doubly reduced form is 2.72 Å, which is smaller than twice the van der Waals radius of the sulfur atom).

For dinuclear complexes **8** and **9**, the first step also occurs as two-electron reduction and is accompanied by deposition of metallic nickel. Apparently, reduction of the complexes of this type is followed by decomposition (see Scheme 14). The formation of amine is confirmed by the presence of an oxidation peak at 0.76 V in the anodic branch of the CV curve. The intensity of this peak increases with accumulation at the potential of the first reduction wave, the increase being particularly substantial for compounds **9**. This peak also appears with time during storage of solutions of complexes **8** and **9** in DMF, which can be attributed to slow displacement of diamines from the coordination sphere of nickel with coordinating solvent molecules. Apparently, the second reduction wave corresponds to reduction of anion **1**⁻ (see Scheme 9 and Table 6). It should be noted that repeated cathodic potential scans lead to shifts of the reduction peaks to less negative values, which may be associated with a loss of the donor amine ligand from the coordination sphere of nickel.

To summarize, we synthesized new Ni^{II} and Co^{III} complexes with thiolate and thione pyrimidine-containing ligands by the reactions of 5-acylpyrimidine-4-thiones with aliphatic diamines in the presence of Ni^{II} and Co^{II} salts. Based on the results of electrochemical study of the complexes, the latter can be divided into the following two types: compounds, which are reduced in the first step without decomposition (compounds **3**, **4**, and **7** with ligand in the anionic thiolate form and containing no chlorine atoms) and compounds, which undergo irreversible two-electron reduction in the first step accompanied by deposition of metallic nickel on the electrode surface (complexes **5**, **6**, **8**, and **9** containing chloride anions).

Experimental

Acetylpyrimidinethiones **1** and **2** were synthesized according to known procedures.^{35,36} The IR spectra were measured on a UR-20 instrument in Nujol mulls. The UV-Vis spectra were recorded on Specord M-40 (200–900 nm) and Nicolet Helios- α (200–1100 nm) instruments in 0.1-cm quartz cells at 20–22 °C. The ^1H NMR spectra were measured on a Varian VXR-400 instrument at 400 MHz. The EI mass spectra were obtained on a JMS-D300 mass spectrometer (direct inlet, the temperature of the ion source was 150 °C, the energy of the ionizing electrons

was 70 eV, the accelerating voltage was 3 kV). The laser-ionization mass spectra were measured on a Bruker Autoflex II time-of-flight mass spectrometer (UV laser, $\lambda = 336$ nm). The presence of isotope signals for all the peaks assigned in the mass spectra confirms the elemental compositions of compounds **3**, **4**, **6**, **8**, and **9**.

Electrochemical studies were carried out on a PI-50-1.1 potentiostat. Glassy-carbon (2 mm in diameter), Pt (3 mm), or Au (1 mm) disks were used as the working electrodes; a 0.05 M Bu_4NClO_4 solution in DMF served as the supporting electrolyte; Ag/AgCl/KCl(satur.) was used as the reference electrode. All measurements were carried out under argon; the samples were dissolved in the pre-deaerated solvent. Dimethylformamide (high-purity grade) was purified by successive refluxing and vacuum distillation over anhydrous CuSO_4 and P_2O_5 .

The experimental intensities of diffraction reflections were measured at room temperature on a single-crystal automated CAD-4 diffractometer³⁷ (Cu- $K\alpha$ radiation, graphite monochromator, ω -scanning technique). The unit cell parameters were determined and refined using 25 reflections in the θ angle range of 26.44–38.57°. The experimental data were processed using the WinGX program package.³⁸ The absorption correction was applied with the use of the ψ -scan method³⁹ based on six selected reflections. The crystal structure was solved by the Patterson method using the DIRDIF-96 program⁴⁰ and refined with anisotropic displacement parameters for all nonhydrogen atoms using the SHELXL-97 program package.⁴¹ In the refinement, the Friedel pairs were not averaged, and the absolute configuration was determined based on the Flack parameter⁴² (–0.026(7)). The positions of the hydrogen atoms were calculated geometrically and refined using a riding model. The atomic coordinates were deposited with the Cambridge Structural Database.

Synthesis of complexes with ligands of the 5-acylpyrimidine-4-thione series (general procedure). *A.* A solution of eda or 1,3-diaminopropane (1 mmol) in EtOH (5 mL) was added with stirring to a suspension of 5-acetylpyrimidine-4-thione **1** or **2** (2 mmol) in EtOH (5–7 mL). After 2–3 min, the precipitate was dissolved. The solution was heated to boiling, after which a hot solution of $\text{NiCl}_2 \cdot 6\text{H}_2\text{O}$ or $\text{CoCl}_2 \cdot 6\text{H}_2\text{O}$ (1 mmol) in a minimum amount of EtOH was added. The reaction mixture was refluxed for 10–30 min and then cooled to 20 °C. The precipitate that formed was filtered off, washed with ethanol, and dried using a water jet vacuum pump at 40–60 °C. If cooling did not lead to precipitation, the reaction mixture was concentrated *in vacuo* to 1/3 of the initial volume and allowed to crystallize at 0 °C for 12 h.

B. The salt $\text{NiCl}_2 \cdot 6\text{H}_2\text{O}$ (2 mmol) was added to a suspension of 5-acetylpyrimidine-4-thione **1** (2 mmol) in EtOH (5–7 mL). The solution was brought to boiling and refluxed for 1 h. Then a hot solution of eda or 1,3-diaminopropane (2 mmol) in EtOH (5 mL) was added and the mixture was refluxed for 0.5–1 h. The product was isolated as described in method *A*.

***N,N'*-Ethylenebis[5-(4-methyl-2-phenyl-6-thiolatopyrimidine)methylketimino]nickel(II) (3).** Compound **3** was prepared from 5-acetylpyrimidine-4-thione **1** (0.5 g, 2 mmol), $\text{NiCl}_2 \cdot 6\text{H}_2\text{O}$ (0.24 g, 1 mmol), and eda (0.06 g, 1 mmol) according to method *A* in a yield of 0.22 g (38%). ¹H NMR (DMSO- d_6), δ : 8.40 and 8.20 (both m, 2 H each, H arom.); 7.45 (m, 6 H, H arom.); 2.30 and 2.45 (both s, 3 H each, Me); 1.40 (br.s, 4 H, H_2CN).

After crystallization of **3**, the mother liquor was concentrated to 1/2 of the initial volume and cooled to 0 °C. A nonidentified brown-red compound crystallized in a yield of 0.20 g. According to elemental analysis, the composition of the latter is identical to that of complex **3** (m.p. 240–242 °C, decomp.).

Bis[*N,N'*-ethylenebis[5-(4-methyl-2-phenyl-6-thiolatopyrimidine)methylketimino]cobalt(III)] peroxide (4). Compound **4** was prepared from 5-acetylpyrimidine-4-thione **1** (0.5 g, 2 mmol), $\text{NiCl}_2 \cdot 6\text{H}_2\text{O}$ (0.24 g, 1 mmol), and eda (0.06 g, 1 mmol) according to method *A* in a yield of 0.21 g (37%). ¹H NMR (DMSO- d_6), δ : 8.25 (d, 2 H, H arom.); 8.20 (m, 2 H, H arom.); 7.42 (m, 6 H, H arom.); 2.30 and 2.45 (both s, 3 H each, Me); 1.60 (br.s, 4 H, HCN).

***N,N'*-1,3-Trimethylenebis[5-(4-methyl-6-phenyl-4-thionopyrimidine)methylketimino]nickel(II) dichloride (5).** Compound **5** was prepared from 5-acetylpyrimidine-4-thione **1** (0.5 g, 2 mmol), $\text{NiCl}_2 \cdot 6\text{H}_2\text{O}$ (0.24 g, 1 mmol), and 1,3-diaminopropane (0.075 g, 1 mmol) according to method *A* in a yield of 0.41 g (63%).

Triaqua-*N,N'*-ethylenebis[5-(2,6-dimethyl-4-thionopyrimidine)methylketimino]nickel(II) dichloride (6). Compound **6** was prepared from 5-acetylpyrimidine-4-thione **2** (0.5 g, 2.7 mmol), $\text{NiCl}_2 \cdot 6\text{H}_2\text{O}$ (0.31 g, 1.3 mmol), and eda (0.08 g, 1.3 mmol) according to method *A* in a yield of 0.30 g (40%).

***fac*-Tris(5-acetyl-2,4-dimethylpyrimidine-6-thiolato)cobalt(III) (7).** Compound **7** was prepared from 5-acetylpyrimidine-4-thione **2** (0.5 g, 2.7 mmol), eda (0.08 g, 1.3 mmol) or 1,3-diaminopropane (0.096 g, 1.3 mmol), and $\text{CoCl}_2 \cdot 6\text{H}_2\text{O}$ (0.31 g, 1.3 mmol) according to method *A* in a yield of 0.20–0.23 g (~60%). ¹H NMR (CDCl_3), δ : 2.65, 2.52, and 2.05 (all s, 9 H each, Me).

The reaction of 5-acetylpyrimidine-4-thione **2**, eda, and $\text{CoCl}_2 \cdot 6\text{H}_2\text{O}$ in deaerated ethanol under Ar afforded a brown-beige product, *viz.*, the $\text{Co}(\text{eda})_2\text{Cl}_2$ complex, in 47% yield. Found (%): C, 19.36; H, 6.35; N, 21.98. $\text{C}_4\text{H}_{16}\text{Cl}_2\text{CoN}_4$. Calculated (%): C, 19.21; H, 6.45; N, 22.41.

Bis[(5-acetyl-2,4-dimethylpyrimidine-6-thiolato)(ethylenediamino)nickel(II) chloride] (8). Compound **8** was prepared from 5-acetylpyrimidine-4-thione **1** (0.5 g, 2 mmol), $\text{NiCl}_2 \cdot 6\text{H}_2\text{O}$ (0.24 g, 1 mmol), and eda (0.06 g, 1 mmol) according to method *B* in a yield of 0.32 g (63%).

Bis[(5-acetyl-2,4-dimethylpyrimidine-6-thiolato)(1,3-propanediamino)nickel(II) chloride] (9). Compound **9** was prepared from 5-acetylpyrimidine-4-thione **1** (0.5 g, 2 mmol), $\text{NiCl}_2 \cdot 6\text{H}_2\text{O}$ (0.24 g, 1 mmol), and 1,3-diaminopropane (0.075 g, 1 mmol) according to method *B* in a yield of 0.25 g (60%).

This study was financially supported by the Russian Foundation for Basic Research (Project No. 04-03-32845), the Program "Russian Universities" (Grant 05.03.046), and the Presidium of the Russian Academy of Sciences (Program "Theoretical and Experimental Studies of the Nature of Chemical Bonds and Mechanisms of Chemical Reactions and Processes").

References

1. K. P. Butin, A. A. Moiseeva, E. K. Beloglazkina, Yu. B. Chudinov, A. A. Chizhevskii, A. V. Mironov, B. N. Tarasevich, A. V. Lalov, and N. V. Zyk, *Izv. Akad. Nauk*,

- Ser. Khim.*, 2005, 169 [*Russ. Chem. Bull., Int. Ed.*, 2005, **54**, 173].
- E. S. Raper, *Coord. Chem. Rev.*, 1985, **61**, 115.
 - I. P. Evans and G. Wilkinson, *J. Chem. Soc., Dalton Trans.*, 1974, 946.
 - E. L. Hegg, *Acc. Chem. Res.*, 2004, **37**, 775.
 - R. P. Hausinger, *J. Biol. Inorg. Chem.*, 1997, **2**, 279.
 - A. Volbeda, M.-H. Charon, E. C. Piras, M. Frey, and J. C. Fontecilla-Camps, *Nature*, 1995, **373**, 580.
 - T. I. Doukov, T. M. Iverson, J. Seravalli, S. W. Ragsdale, and C. L. Drennan, *Science*, 2002, **298**, 567.
 - E. S. Raper, *Coord. Chem. Rev.*, 1996, **153**, 199.
 - A. R. Katrizly, K. Jug, and D. C. Oniciu, *Chem. Rev.*, 2001, **101**, 1421.
 - D. Moran, K. Sukcharoenphon, R. Puchta, H. F. Schaefer, P. V. R. Schleyer, and C. D. Hoff, *J. Org. Chem.*, 2002, **67**, 9061.
 - M. D. Couce, U. Russo, and G. Valle, *Inorg. Chim. Acta*, 1995, **234**, 195.
 - E. S. Raper, *Coord. Chem. Rev.*, 1997, **165**, 475.
 - C. Chieh, *Can. J. Chem.*, 1976, **56**, 560.
 - P. D. Cookson and E. R. T. Tiekink, *J. Chem. Soc., Dalton Trans.*, 1993, 259.
 - I. P. Evans and G. Wilkinson, *J. Chem. Soc., Dalton Trans.*, 1974, 946.
 - A. L. Nivorozhkin, H. Toftlund, and M. Nielsen, *J. Chem. Soc., Dalton Trans.*, 1994, 361.
 - S. Knoblauch, R. Benedix, M. Ecke, T. Gelbrich, T. Sieler, F. Somoza, and H. Hennig, *Eur. J. Inorg. Chem.*, 1999, 1393.
 - O. P. Anderson, J. Becher, H. Frydendahl, L. F. Taylor, and H. Toftlund, *Chem. Commun.*, 1986, 699.
 - A. E. Mistryukov, I. S. Vasil'chenko, V. S. Sergienko, A. L. Nivorozhkin, S. G. Kochin, M. A. Porai-Koshits, L. E. Nivorozhkin, and A. D. Garmovskii, *Mendeleev Commun.*, 1992, 30.
 - A. La Cour, H. Toftlund, K. S. Murray, and E. R. T. Tiekink, *Z. Kristallogr. — New Cryst. Struct.*, 2002, **217**, 215.
 - L. Hennig, R. Kirmse, O. Hammerich, S. Larsen, H. Fridendahl, H. Toftlund, and J. Becher, *Inorg. Chim. Acta*, 1995, **234**, 67.
 - B. A. Cartwright, P. O. Langguth, Jr., and A. C. Skapski, *Acta Crystallogr., Sect. B: Struct. Crystallogr. Cryst. Chem.*, 1979, **35**, 63.
 - B. A. Cartwright, D. M. L. Goodgame, I. Jeeves, P. O. Langguth, and A. C. Skapski, *Inorg. Chim. Acta*, 1977, **24**, L45; S. Seth, *Acta Crystallogr., Sect. C*, 1994, **50**, 1196.
 - E. C. Constable, C. A. Palmer, and D. A. Tocher, *Inorg. Chim. Acta*, 1990, **176**, 57.
 - E. Block, H. Kang, G. Ofori-Okai, and J. Zubieta, *Inorg. Chim. Acta*, 1991, **188**, 61.
 - J. K. Burdett, *Inorg. Chem.*, 1976, **15**, 212.
 - J. J. P. Stewart, *J. Comput. Chem.*, 1989, **10**, 209.
 - E. K. Beloglazkina, A. A. Moiseeva, A. V. Churakov, I. S. Orlov, N. V. Zyk, J. A. K. Howard, and K. P. Butin, *Izv. Akad. Nauk, Ser. Khim.*, 2002, 436 [*Russ. Chem. Bull., Int. Ed.*, 2002, **51**, 467].
 - M. Ghiladi, J. T. Gomes, A. Hazell, P. Kofod, J. Lumtscher, and C. J. McKenzie, *J. Chem. Soc., Dalton Trans.*, 2003, 1320.
 - E. Szlyk, S. Biniak, and E. Larsen, *J. Solid State Electrochem.*, 2001, **5**, 221.
 - A. Andreev, V. Ivanova, L. Prahov, and I. D. Schopov, *J. Mol. Catal., A: Chem.*, 1995, **95**, 197.
 - G. N. Schrauzer and R. J. Windgassen, *Chem. Ber.*, 1966, **99**, 602.
 - A. M. Bond, *Modern Polarographic Methods in Analytical Chemistry*, Marcell Dekker, New York, 1980.
 - A. Ulman, *Chem. Rev.*, 1996, **96**, 1533.
 - J. Goerdeler and H. Pohland, *Chem. Ber.*, 1963, **96**, 526.
 - J. Goerdeler and U. Keuser, *Chem. Ber.*, 1964, **97**, 3106.
 - Enraf—Nonius. CAD-4 Software. Version 5.0*, Enraf—Nonius, Delft, The Netherlands, 1989.
 - L. J. Farrugia, *J. Appl. Crystallogr.*, 1999, **32**, 837.
 - A. C. T. North, D. C. Phillips, and F. S. Mathews, *Acta Crystallogr., Sect. A*, 1968, **24**, 351.
 - P. T. Beurskens, G. Beurskens, W. P. Bosman, R. de Gelder, S. Garcia-Granda, R. O. Gould, R. Israel, and J. M. M. Smits, *The DIRDIF-96 Program System. Technical Report*, Crystallography Laboratory, University of Nijmegen, The Netherlands, 1996.
 - G. M. Sheldrick, *SHELXL-97, Program for the Refinement of Crystal Structures*, University of Göttingen, Göttingen, Germany, 1997.
 - H. D. Flack, *Acta Crystallogr., Sect. A*, 1983, **39**, 876.

Received May 20, 2005;
in revised form August 25, 2005